

Interpreting Latent Spaces of Generative Models for Medical Images using Unsupervised Methods

Julian Schön¹

Raghavendra Selvan^{1,2}

Jens Petersen^{1,3}

JULIAN.E.S@DI.KU.DK

RAGHAV@DI.KU.DK

PHUP@DI.KU.DK

¹ *Department of Computer Science, University of Copenhagen, Denmark*

² *Department of Neuroscience, University of Copenhagen, Denmark*

³ *Department of Oncology, Rigshospitalet, Denmark*

Editors: Under Review for MIDL 2022

Abstract

Generative models such as Generative Adversarial Networks (GANs) and Variational Autoencoders (VAEs) play an increasingly important role in medical image analysis. They are used to synthesize, de-noise, super-resolve, and augment medical images. The latent spaces of these models often show semantically meaningful directions corresponding to human-interpretable image transformations. However, until now, their exploration for medical images has been limited due to the requirement of supervised data. Recently, several methods for unsupervised discovery of interpretable directions in GAN latent spaces have shown interesting results on natural images. This work explores the potential of applying these techniques on medical images by training a deep convolutional GAN and a VAE on thoracic CT scans and using an unsupervised method to discover interpretable directions in the resulting latent space. We find several directions corresponding to non-trivial image transformations, such as rotation or breast size, as well as directions showing that the generative models capture 3D structure despite being presented only with two-dimensional data. The results show that unsupervised methods to discover interpretable directions in generative model latent spaces generalize to VAEs and can be applied to medical images. This could open a wide array of future work using these methods in medical image analysis.

Keywords: Generative models, unsupervised learning, interpretability, CT

1. Introduction

The combination of deep learning and medical images has emerged as a promising tool for diagnostics and treatment. Though the amount of available data is increasing, one of the main limitations is the often small dataset sizes available to learn from. This is due to reasons such as the high costs of collecting and labeling data, adverse effects of radiation exposure from imaging procedures, and protection of sensitive patient data. Generative models can be used to synthesize or augment medical images (Nie et al., 2017; Frid-Adar et al., 2018; Hiasa et al., 2018; Zhu et al., 2019), mitigating some of these factors.

Generative Adversarial Networks (GANs) (Goodfellow et al., 2014) have emerged as the prominent generative model for image synthesis in recent years. Consequently, an extensive line of research focusing on the interpretability of GANs has unfolded. Lately, there has been a focus on the structure and interpretability of the latent space learned by GANs. Radford et al. (2016) showed that there is meaningful vector arithmetic in the latent space

of Deep Convolutional Generative Adversarial Networks (DCGANs). This led to the investigation of interpretable directions in GAN latent spaces. For several years, the methods used for discovering interpretable directions in latent spaces have been supervised (Goetschalckx et al., 2019; Shen et al., 2020; Jahanian et al., 2020; Plumerault et al., 2020). Especially in medical image analysis, supervision is expensive as it typically involves radiologist’s or other expert’s time. Recently, several unsupervised methods for the discovery of interpretable directions in GAN latent spaces were presented (Voynov and Babenko, 2020; Härkönen et al., 2020; Shen and Zhou, 2021). Since these methods do not require supervision, they seem more promising for the medical domain. However, at present it is unclear if they work with the often more homogeneous images and the smaller dataset sizes encountered in this field. Variational Autoencoders (VAEs) (Kingma and Welling, 2014) are another popular class of generative models that explicitly approximate the data distribution (Goodfellow, 2016). Research on the interpretability of VAEs has mainly focused on obtaining disentangled latent space representations (Higgins et al., 2017; Kim and Mnih, 2018). While this shows promising results, there are limitations to unsupervised learning of disentangled representations, in that it might not be possible without introducing inductive biases (Locatello et al., 2019). The approach of Voynov and Babenko (2020), does not restrict the latent space representation as it is trained post-hoc. Thus, this and similar methods developed for GANs, when applied to VAEs, allow for latent spaces that need not incorporate additional inductive biases. This allows for easier applications of discovered directions to real images. If the same methods that have shown promising results on GANs are effective on VAEs, then VAEs can be trained without restrictions on the latent space while still having the benefit of interpretability and applicability to real images.

Contributions: We employ an unsupervised technique to explore the latent spaces of DCGANs and VAEs trained on Computed Tomography (CT) images¹. We show that these methods previously used to interpret the latent spaces of GANs generalizes to VAEs. Further, our results provide insights into the applicability of these methods for medical image analysis. We evaluate the directions obtained and show that there are non-trivial and semantically meaningful directions encoded in the latent space of the generative models under consideration. These directions include both transformations specific to our dataset choice and ones that likely generalize to other data.

2. Background

2.1. Generative Adversarial Networks

GANs (Goodfellow et al., 2014) are a class of deep generative models that implicitly model the data generating distribution (Goodfellow, 2016). They optimize a zero-sum game between a generator neural network that synthesizes new data from random samples and a discriminator neural network that classifies real and synthesized data. The generator, $G : z \in \mathbb{R}^L \rightarrow x \in \mathcal{D}$, maps from a L -dimensional latent variable z to the data space \mathcal{D} . The discriminator, $D : x \in \mathcal{D} \rightarrow \{0, 1\}$, presented with $G(z)$ and real samples, is tasked with classifying them as real or fake.

Given the latent distribution p_z , the data distribution p_{data} , and binary cross-entropy as

1. <https://github.com/julschoen/Latent-Space-Exploration-CT>

the loss we can define the min-max game as:

$$\min_G \max_D V(D, G) = \mathbb{E}_{x \sim p_{data}} [\log D(x)] + \mathbb{E}_{z \sim p_z} [\log(1 - D(G(z)))]. \quad (1)$$

The introduction of DCGANs (Radford et al., 2016) has increased the use of GANs on images. In particular, there is a vast amount of work showing their effectiveness in medical imaging (Zhang et al., 2018; Diaz-Pinto et al., 2019; Alyafi et al., 2020; Bushra and Shobana, 2020; Fujioka et al., 2019).

2.2. Variational Autoencoders

VAEs (Kingma and Welling, 2014) are another popular class of deep latent variable models used for generative modelling and approximating the data generating distribution explicitly (Goodfellow, 2016). The standard VAE uses a probabilistic encoder-decoder architecture. The probabilistic encoder, parameterised by θ , is given by $q_\theta(\cdot) : x \in \mathcal{D} \mapsto z \in \mathbb{R}^L$, where z is the L -dimensional latent variable. The encoder approximates the true posterior distribution, $p(z|x)$, with a Gaussian density with mean $\mu_\theta \in \mathbb{R}^L$ and variance $\sigma_\theta^2 \in \mathbb{R}^L$, i.e., $q_\theta(z|x) \sim \mathcal{N}(\mu_\theta, \sigma_\theta^2)$. The decoder, given by $p_\phi(x|z)$ and parameterised by ϕ , is trained to reconstruct the input x based on the latent variable z .

The VAE is optimized using the Evidence Lower Bound (ELBO) as the objective (Kingma and Welling, 2014). The ELBO is given by:

$$\mathcal{L}_{VAE} = -\mathbb{E}_{q_\theta} [\log p_\phi(x|z)] + D_{KL}[q_\theta(z|x)||p(z)] \quad (2)$$

where the first term is referred to as the reconstruction loss \mathcal{L}_{rec} , and the second term as the regularization loss \mathcal{L}_{reg} given by the Kullback-Leibler Divergence (KLD) and $p(z)$ is the prior given by $p(z) \sim \mathcal{N}(\mathbf{0}, \mathbf{I})$. The regularization loss forces the encoder density to match the prior during training, enabling generative sampling from the prior density at inference. To balance latent space regularization and reconstruction quality, an additional scaling factor β , suggested by Higgins et al. (2017), is introduced, giving:

$$\mathcal{L}_{VAE} = \mathcal{L}_{rec} + \beta \mathcal{L}_{reg} \quad (3)$$

VAEs often suffer from 'posterior collapse' (Bowman et al., 2016; Kingma et al., 2016) which can be alleviated when using a $\beta < 1$.

2.3. Unsupervised Discovery of Interpretable Directions in Latent Spaces

Recently, several unsupervised methods to find interpretable directions in GAN latent spaces have been proposed (Voynov and Babenko, 2020; Härkönen et al., 2020; Shen and Zhou, 2021). In Härkönen et al. (2020); Shen et al. (2020) the interpretable directions are constrained to be orthogonal, whereas this constraint is relaxed in Voynov and Babenko (2020). As interpretable directions do not necessarily have to be orthogonal, we employ the method suggested by Voynov and Babenko (2020). The proposed method is model agnostic and can be applied to any latent generative model G . The goal of this unsupervised method is to learn distinct directions from a trained latent generative model, by learning a directions matrix A and a reconstructor R to distinguish between the directions. Since the method

jointly learns a set of directions and a model that distinguishes the resulting transformations, the directions are likely to be interpretable if the model can distinguish between them with high accuracy. If the directions do not affect all images the same or are semantically not meaningful, distinguishing them would be hard.

Formally, the unsupervised direction discovery method learns two things: First, a matrix $A \in \mathbb{R}^{d \times K}$, where d is the dimensionality of the latent space of G , and K is the number of directions that will be discovered. I.e., the columns of A correspond to the directions. Second, a reconstructor R , mapping from an image pair $(G(z), G(z + A(\epsilon e_k)))$, with the shifted latent vector $z + A(\epsilon e_k)$, where e_k is an axis-aligned unit vector and ϵ is a scalar. The reconstructor predicts the direction k by determining e_k and the scalar ϵ . In other words, the reconstructor is given an image and a shifted version and tries to determine the amount, and direction of the shift. The optimization objective is given by:

$$\min_{A,R} \mathbb{E}_{z,k,\epsilon} [L_{cl}(k, \hat{k}) + \gamma L_s(\epsilon, \hat{\epsilon})] \quad (4)$$

where k and ϵ are the actual direction and amount respectively, and \hat{k} and $\hat{\epsilon}$ are the predictions, L_{cl} is the classification loss based on the Reconstructor Classification Accuracy (RCA), L_s is the shift loss, and γ is a regularization factor.

3. Material & Methods

3.1. Data

We use The Lung Image Database Consortium image collection (LIDC-IDRI) (Armato III et al., 2011) provided by The Cancer Imaging Archive (TCIA). It consists of clinical thoracic CT scans of 1010 patients, collected from diagnostic and lung cancer screenings and is assembled by seven academic centers and eight medical imaging companies. We consider each axial CT slice as an individual image. This results in a dataset of 246,016 512×512 pixel CT images, which are resized to 128×128 pixels to limit computational demands.

3.2. Models & Training

We use a DCGAN based on Radford et al. (2016), improving training stability by introducing one-sided label smoothing (Salimans et al., 2016). One-sided label smoothing replaces the fixed targets 1 of the real labels with smoothed values randomly chosen from the interval $[0.9, 1]$. Additionally, we add 0-mean and 0.1 standard deviation Gaussian noise to the discriminator input (Arjovsky and Bottou, 2017), incrementally reducing the standard deviation and finally removing it at epoch 25. The encoder and decoder of the VAE are based on ResNet (He et al., 2016), and we use $\beta = 0.01$ to improve reconstruction quality. For both generative models, we use a latent space size of $L = 32$ as it showed the best trade-off between image quality and compactness of the latent space. We refer to the provided GitHub repository for implementation details. We train the GAN and the VAE for 50 epochs selecting the best weights out of the last 5 by considering the models Fréchet Inception Distance (FID) (Heusel et al., 2017) on test data. We use binary cross-entropy as loss for the GAN and log mean squared error (Yu, 2020) as reconstruction loss for the VAE. We use Adam (Kingma and Ba, 2015) with a learning rate of 0.0002 and 0.0001 to optimize

the GAN and VAE, respectively. The best GAN and VAE weights yield a FID of 33.4 on and 93.9 on the test data, respectively. Appendix C offers a short study of memorization. To find interpretable latent directions, we use two different reconstructors, based on LeNet (Lecun et al., 1998) and ResNet. We experiment with A having unit length or orthonormal columns as suggested by Voynov and Babenko (2020). We set the number of directions K equal to the size of the latent space, i.e., $K = 32$, and experiment with increasing it to $K = 100$. We observe significantly faster convergence when using the ResNet reconstructor. Thus, when using $K = 32$, we train the model for 25,000 iterations when using LeNet and 3,000 iterations when using the ResNet reconstructor. When $K = 100$, we train the VAE for 75,000 and 4,000 iterations with the LeNet and ResNet reconstructors respectively. For the GAN we observe slower convergence. Therefore, we train the GAN for 250,000 and 10,000 iterations with the LeNet and ResNet reconstructors, respectively. Since we cannot have $K > L$ for orthonormal directions, we only use A with columns of unit length for $K = 100$. We evaluate direction models using the RCA and the shift loss L_s from Equation 4. Further, we follow the ablation provided by Voynov and Babenko (2020) and use a regularization factor $\gamma = 0.25$. To evaluate the directions, preliminary labeling was done by the first author with eight animations, each showing different latent vectors per direction. Next, each direction and preliminary label was considered on eight static images. The evaluator does not have formal training in medical image interpretation, and it is possible that more experienced evaluators could have discovered more interesting directions.

4. Experiments & Results

We perform several experiments to investigate the unsupervised exploration of latent spaces of deep generative models. First, we train using orthonormal directions and directions of unit length. We also experiment with increasing the number of directions. Finally, we perform all experiments both with a DCGAN and a VAE as generative model.

All results are obtained without supervision, with the exception of the labeling of the selected directions. The RCA and L_s of the different experiments are presented in Tables 1(b) and 1(a) for the LeNet and ResNet reconstructors respectively. There are several key

Table 1: Reconstructor Classification Accuracy (RCA) and L_s for all model configurations for ResNet (a) and LeNet (b) as reconstructor.

(a) RCA and L_s for ResNet reconstructor.						
	Orthogonal		Unit Length		100 Directions	
	RCA	L_s	RCA	L_s	RCA	L_s
GAN	0.9236	0.2538	0.9383	0.1949	0.9522	0.1560
VAE	0.9939	0.1040	0.9947	0.1086	0.9861	0.1117

(b) RCA and L_s for LeNet reconstructor.						
	Orthogonal		Unit Length		100 Directions	
	RCA	L_s	RCA	L_s	RCA	L_s
GAN	0.8559	0.3317	0.9062	0.2439	0.9305	0.1406
VAE	0.9800	0.1421	0.9895	0.1090	0.9791	0.0962

observations. First, the VAE always outperforms the GAN with respect to both RCA and L_s . Second, using directions of unit length achieves higher RCA than orthonormal directions and lower L_s in all but one case. We also observe higher RCA when using ResNet over LeNet as a reconstructor. In contrast, LeNet achieves a lower L_s when K is set to 100. Voynov and Babenko (2020) mention that a larger K does not harm interpretability but alleviates entanglement, and may, lead to more duplicate directions. We observe the same behaviour with $K = 100$ as opposed to $K = 32$.

We consistently observe eight key directions in our results. Namely, width, height, size, y -translation, rotation, breast size, thickness, and z -Position. All model configurations find all eight directions with varying degrees of entanglement. In this work, we omit directions entangled to such a degree that there is no clear interpretation dominating the image transformation. Thus, all configurations find at least a subset of the aforementioned directions in a sufficiently disentangled manner. We present animations of all discovered directions in the provided GitHub repository. Figures 1(a) and 1(b) show all eight directions for the VAE and GAN respectively. The directions presented in Figure 1 are obtained using LeNet as reconstructor and $K = 100$. For images of the other model configurations, we refer to Appendix A. Our results show that enforcing orthonormal directions increases entanglement.

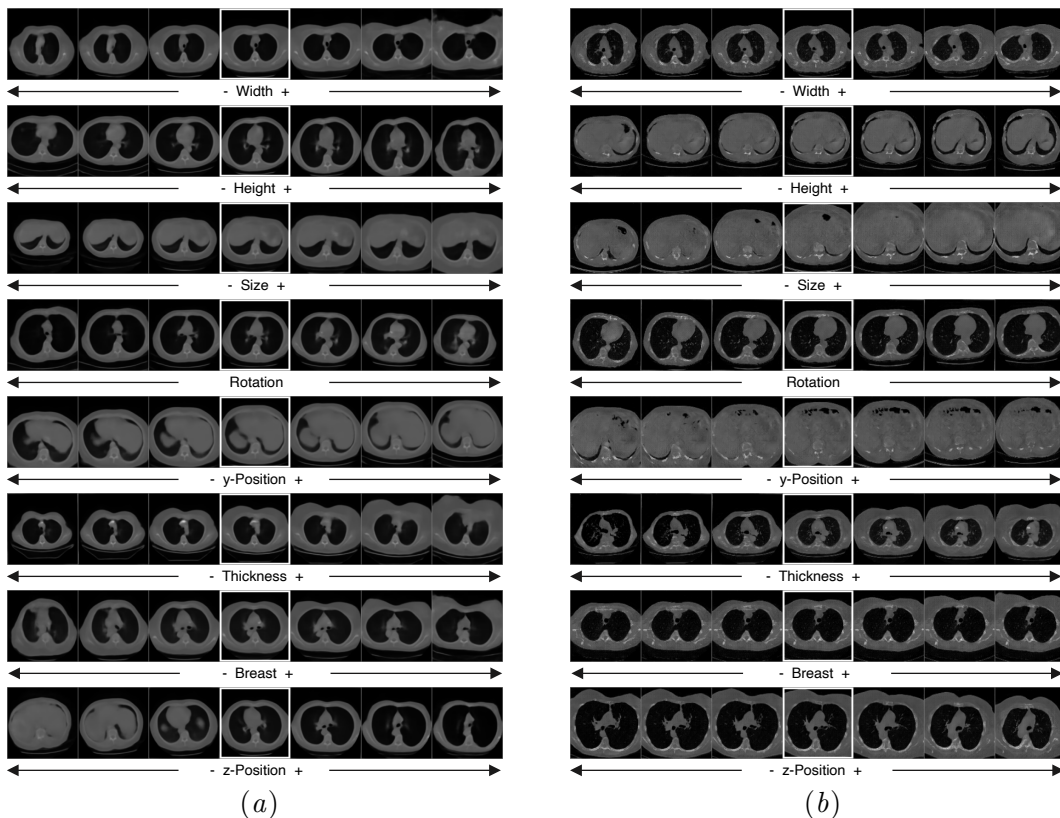


Figure 1: Interpretable directions using $A^{32 \times 100}$ with columns of unit length, LeNet as reconstructor, and the VAE (a) and GAN (b) as underlying generative models. The central images correspond to the original latent vector. The left/right images correspond to shifts.

Finally, we observe that when using a LeNet reconstructor, more of the obtained directions are easily interpretable compared to using a ResNet reconstructor.

5. Discussion

In this work, we explored the latent spaces of deep generative models, such as GANs and VAEs, to discover semantically meaningful directions. We next elaborate on some of the findings from our experiments.

Influence of K : The main effects of variations in the number of directions, K , is that lower K likely makes the reconstructor classification task easier. It is possible that this lessens the need for disentanglement. If so, when increasing K to 100, the increasing classification difficulty forces the model to disentangle the directions to make them easier to classify.

Orthonormal Directions: While constraining the directions to be orthonormal still leads to the same subset of interpretable directions being discovered, the quality of the directions suffers. This aligns with the observations of [Voynov and Babenko \(2020\)](#). However, their results show that some datasets benefit from orthonormal directions, leading to more interesting directions. We do not observe this on our data, and the lack of disentanglement is also clear from the lower RCA of the methods using orthonormal directions. Thus, we conclude that for our purpose, directions of unit length are preferable.

Choice of Reconstructor: When $K = 32$ both reconstructors show similar qualitative results, more entangled directions, L_s is larger and ResNet quantitatively outperforms LeNet. For $K = 100$, LeNet produces better qualitative results than ResNet. This is also evident in the quantitative results with LeNet and $K = 100$ achieving the lowest L_s . While ResNet has a higher RCA, RCA gives a measure of duplicate directions and only describes interpretability to a certain degree. Since LeNet performed best when using $K = 100$ and the increased number of directions benefited disentanglement we prefer LeNet as reconstructor.

Consistent Discovery of the Same Human Interpretable Directions: The same subset of interpretable directions appears for all models with varying degree of entanglement. Recent work has shown non-linear directions to be less entangled ([Tzelepis et al., 2021](#)) which could be studied further. The directions are validated by showing that the same set is discovered in the latent space of both the DCGAN and the VAE as shown in [Figure 1](#). The resulting directions we discover show non-trivial image transformations. In particular, the directions changing the z -Position of the latent vector are interesting. It demonstrates that the models learn the 3-dimensional structure of the data despite being trained on 2-dimensional images. We provide further illustrations of the z -Position changes and a comparison of random directions with the discovered directions in [Appendix B](#).

While the focus of discovery of directions in latent spaces has mainly been on GANs in recent years, we see that the same methods apply to VAEs. Since VAEs allow for easy mapping of real images to latent vectors, they have a practical benefit over GANs when considering the usefulness of these methods as covered in the following.

Impact & Applications: Improving interpretability of GANs and VAEs is important and addressed in this work by finding and visualizing meaningful latent space directions and providing novel insights into the learned representations. The method is shown to generalize to VAEs, indicating that the latent spaces of VAEs and GANs can be interpreted in similar ways. However, shorter convergence times on the VAE when learning interpretable direc-

tions indicate that VAEs latent space could be inherently easier to interpret. Unsupervised exploration further benefits the medical image domain due to the lack of well-supervised datasets and more importantly, it could lead to surprising results outside of what we are explicitly supervising methods to find.

Context-aware image augmentation and editing is another application of our approach. Image augmentation using synthetic data improves downstream machine learning tasks on medical images over standard augmentation methods (Frid-Adar et al., 2018; Sandfort et al., 2019; Ge et al., 2020; Shin et al., 2018; Chaitanya et al., 2021) and GANs can alleviate both the small dataset sizes and imbalance inherent to medical imaging (Kazemnia et al., 2020; Yi et al., 2019). Our results could be used to explore more diverse augmentations and the capability of adjusting for sex and weight imbalances. A recent supervised approach explored disease-aware image editing (Saboo et al., 2021), alleviating class imbalances. Our work might offer an alternate unsupervised approach. Using VAEs or reverse latent vector search (Fernández Blanco et al., 2021) allows for image editing and augmentation.

We see further applications needing more investigation, such as exploring the potential in consistency regularization and multi-modal datasets. For example, finding directions corresponding to adding or removing contrast in scans. Further, the approach we use has been shown to be effective in unsupervised saliency detection, and segmentation on natural images (Voynov et al., 2021; Melas-Kyriazi et al., 2021; Voynov and Babenko, 2020).

Limitations: The main limitations we observe in our work are based on the methodology for unsupervised exploration. First, while the reconstructor’s classification accuracy and shift loss give some insights into convergence, the implications of overfitting need to be investigated further. In particular, since the method does not rely on data, techniques such as evaluation of hold-out data are not available. This makes the decision of how many training iterations to use difficult as model performance can not be assessed on independent data. Further, the lack of evaluation metrics makes the choice of reconstructor difficult. We tried to mitigate this by using RCA and L_s for quantitative and human interpretation for qualitative analysis. Nevertheless, further investigation is needed to find good evaluation metrics. Second, the large amount of resulting directions makes evaluation difficult and time-consuming. This is particularly challenging in medical image analysis as evaluation may need to involve trained evaluators such as radiologists. Further automation or introducing a hierarchy of interpretability could be a focus of future work.

6. Conclusion

In this work, we have demonstrated for the first time that techniques for unsupervised discovery of interpretable directions in the latent space of generative models yield good results on medical images and for dataset sizes typically encountered in this field. The results show that generative models, such as a DCGAN and VAE learn non-trivial, semantically meaningful directions when trained on CT images of the thorax. We encounter directions with the same semantic meaning regardless of the generator or direction discovery model, indicating a general structure of the latent spaces. Further, our results show that the latent spaces of the generative models capture the 3D structure of the CT scans despite only being trained on 2D slices. The work opens up the possibility of exploring these techniques for unsupervised medical image segmentation, interpolation, augmentation, and more.

Acknowledgments

The authors acknowledge the National Cancer Institute and the Foundation for the National Institutes of Health, and their critical role in the creation of the free publicly available LIDC/IDRI Database used in this study. The authors would like to thank Anna Kirchner and Arnau Moranchó Tardà for help in preparation of the manuscript. Jens Petersen is partly funded by research grants from the Danish Cancer Society (grant no. R231-A13976) and Varian Medical Systems.

References

- Basel Alyafi, Oliver Diaz, and Robert Marti. Dcgans for realistic breast mass augmentation in x-ray mammography. In *Medical Imaging 2020: Computer-Aided Diagnosis*, volume 11314, pages 473 – 480. International Society for Optics and Photonics, SPIE, 2020. URL <https://doi.org/10.1117/12.2543506>.
- Martín Arjovsky and Léon Bottou. Towards principled methods for training generative adversarial networks. In *5th International Conference on Learning Representations*, 2017. URL https://openreview.net/forum?id=Hk4_qw5xe.
- Samuel G Armato III, Geoffrey McLennan, Luc Bidaut, Michael F McNitt-Gray, Charles R Meyer, Anthony P Reeves, Binsheng Zhao, Denise R Aberle, Claudia I Henschke, Eric A Hoffman, et al. The lung image database consortium (lidc) and image database resource initiative (idri): A completed reference database of lung nodules on ct scans. *Medical physics*, 38(2):915–931, 2011. URL <https://aapm.onlinelibrary.wiley.com/doi/abs/10.1118/1.3528204>.
- Samuel R. Bowman, Luke Vilnis, Oriol Vinyals, Andrew M. Dai, Rafal Józefowicz, and Samy Bengio. Generating sentences from a continuous space. In *Proceedings of the 20th SIGNLL Conference on Computational Natural Language Learning*, pages 10–21. ACL, 2016. URL <https://doi.org/10.18653/v1/k16-1002>.
- S. Nikkath Bushra and G. Shobana. A survey on deep convolutional generative adversarial neural network (dcgan) for detection of covid-19 using chest x-ray/ct-scan. In *3rd International Conference on Intelligent Sustainable Systems*, pages 702–708, 2020. URL <https://ieeexplore.ieee.org/document/9316125>.
- Krishna Chaitanya, Neerav Karani, Christian F. Baumgartner, Ertunc Erdil, Anton S. Becker, Olivio Donati, and Ender Konukoglu. Semi-supervised task-driven data augmentation for medical image segmentation. *Medical Image Analysis*, 68:101934, 2021. URL <https://doi.org/10.1016/j.media.2020.101934>.
- Andres Diaz-Pinto, Adrián Colomer, Valery Naranjo, Sandra Morales, Yanwu Xu, and Alejandro F. Frangi. Retinal image synthesis and semi-supervised learning for glaucoma assessment. *IEEE Transactions on Medical Imaging*, 38(9):2211–2218, 2019. URL <https://doi.org/10.1109/TMI.2019.2903434>.
- Rubén Fernández Blanco, Pilar Rosado, Esteban Vegas, and Ferran Reverter. Medical image editing in the latent space of generative adversarial networks. *Intelligence-Based Medicine*, 5:100040, 2021. URL <https://www.sciencedirect.com/science/article/pii/S2666521221000168>.
- Maayan Frid-Adar, Idit Diamant, Eyal Klang, Michal Amitai, Jacob Goldberger, and Hayit Greenspan. Gan-based synthetic medical image augmentation for increased cnn performance in liver lesion classification. *Neurocomputing*, 321:321–331, 2018. URL <https://www.sciencedirect.com/science/article/pii/S0925231218310749>.
- Tomoyuki Fujioka, Mio Mori, Kazunori Kubota, Yuka Kikuchi, Leona Katsuta, Mio Adachi, Goshi Oda, Tsuyoshi Nakagawa, Yoshio Kitazume, and Ukihide Tateishi. Breast ultrasound image

- synthesis using deep convolutional generative adversarial networks. *Diagnostics*, 9(4), 2019. URL <https://www.mdpi.com/2075-4418/9/4/176>.
- Chenjie Ge, Irene Yu-Hua Gu, Asgeir Store Jakola, and Jie Yang. Enlarged training dataset by pairwise gans for molecular-based brain tumor classification. *IEEE Access*, 8:22560–22570, 2020. URL <https://doi.org/10.1109/ACCESS.2020.2969805>.
- Lore Goetschalckx, Alex Andonian, Aude Oliva, and Phillip Isola. Ganalyze: Toward visual definitions of cognitive image properties. In *IEEE/CVF International Conference on Computer Vision*, pages 5743–5752, 2019. URL <https://ieeexplore.ieee.org/document/9010379>.
- Ian J. Goodfellow. NIPS 2016 tutorial: Generative adversarial networks. 2016. URL <http://arxiv.org/abs/1701.00160>.
- Ian J. Goodfellow, Jean Pouget-Abadie, Mehdi Mirza, Bing Xu, David Warde-Farley, Sherjil Ozair, Aaron C. Courville, and Yoshua Bengio. Generative adversarial nets. In *Advances in Neural Information Processing Systems 27: Annual Conference on Neural Information Processing Systems*, pages 2672–2680, 2014. URL <https://proceedings.neurips.cc/paper/2014/hash/5ca3e9b122f61f8f06494c97b1afccf3-Abstract.html>.
- Erik Härkönen, Aaron Hertzmann, Jaakko Lehtinen, and Sylvain Paris. Ganspace: Discovering interpretable gan controls. In *Advances in Neural Information Processing Systems*, volume 33, pages 9841–9850. Curran Associates, Inc., 2020. URL <https://tinyurl.com/4rycanab>.
- Kaiming He, Xiangyu Zhang, Shaoqing Ren, and Jian Sun. Deep residual learning for image recognition. In *IEEE Conference on Computer Vision and Pattern Recognition*, pages 770–778. IEEE Computer Society, 2016. URL <https://doi.org/10.1109/CVPR.2016.90>.
- Martin Heusel, Hubert Ramsauer, Thomas Unterthiner, Bernhard Nessler, and Sepp Hochreiter. Gans trained by a two time-scale update rule converge to a local nash equilibrium. In *Advances in Neural Information Processing Systems*, volume 30. Curran Associates, Inc., 2017. URL <https://proceedings.neurips.cc/paper/2017/file/8a1d694707eb0fefe65871369074926d-Paper.pdf>.
- Yuta Hiasa, Yoshito Otake, Masaki Takao, Takumi Matsuoka, Kazuma Takashima, Aaron Carass, Jerry L. Prince, Nobuhiko Sugano, and Yoshinobu Sato. Cross-modality image synthesis from unpaired data using cyclegan. In *Simulation and Synthesis in Medical Imaging*, pages 31–41. Springer International Publishing, 2018. URL https://link.springer.com/chapter/10.1007/978-3-030-00536-8_4.
- Irina Higgins, Loïc Matthey, Arka Pal, Christopher Burgess, Xavier Glorot, Matthew Botvinick, Shakir Mohamed, and Alexander Lerchner. beta-vae: Learning basic visual concepts with a constrained variational framework. In *5th International Conference on Learning Representations*, 2017. URL <https://openreview.net/forum?id=Sy2fzU9gl>.
- Ali Jahanian, Lucy Chai, and Phillip Isola. On the "steerability" of generative adversarial networks. In *8th International Conference on Learning Representations*, 2020. URL <https://openreview.net/forum?id=HylsTT4FvB>.
- Salome Kazemina, Christoph Baur, Arjan Kuijper, Bram van Ginneken, Nassir Navab, Shadi Albarqouni, and Anirban Mukhopadhyay. Gans for medical image analysis. *Artificial Intelligence in Medicine*, 109:101938, 2020. URL <https://doi.org/10.1016/j.artmed.2020.101938>.
- Hyunjik Kim and Andriy Mnih. Disentangling by factorising. In *Proceedings of the 35th International Conference on Machine Learning*, volume 80 of *Proceedings of Machine Learning Research*, pages 2649–2658, 2018. URL <https://proceedings.mlr.press/v80/kim18b.html>.
- Diederik P. Kingma and Jimmy Ba. Adam: A method for stochastic optimization. In *3rd International Conference on Learning Representations*, 2015. URL <http://arxiv.org/abs/1412.6980>.
- Diederik P. Kingma and Max Welling. Auto-encoding variational bayes. In *2nd International Conference on Learning Representations*, 2014. URL <http://arxiv.org/abs/1312.6114>.
- Durk P Kingma, Tim Salimans, Rafal Jozefowicz, Xi Chen, Ilya Sutskever, and Max Welling. Improved variational inference with inverse autoregressive flow. In *Advances in Neural Information*

- Processing Systems*, volume 29. Curran Associates, Inc., 2016. URL <https://proceedings.neurips.cc/paper/2016/file/ddeebdeefdb7e7e7a697e1c3e3d8ef54-Paper.pdf>.
- Y. Lecun, L. Bottou, Y. Bengio, and P. Haffner. Gradient-based learning applied to document recognition. *Proceedings of the IEEE*, 86(11):2278–2324, 1998. URL <https://ieeexplore.ieee.org/document/726791>.
- Francesco Locatello, Stefan Bauer, Mario Lucic, Gunnar Raetsch, Sylvain Gelly, Bernhard Schölkopf, and Olivier Bachem. Challenging common assumptions in the unsupervised learning of disentangled representations. In *Proceedings of the 36th International Conference on Machine Learning*, volume 97 of *Proceedings of Machine Learning Research*, pages 4114–4124, 2019. URL <https://proceedings.mlr.press/v97/locatello19a.html>.
- Luke Melas-Kyriazi, Christian Rupprecht, Iro Laina, and Andrea Vedaldi. Finding an unsupervised image segmenter in each of your deep generative models. 2021. URL <https://arxiv.org/abs/2105.08127>.
- Dong Nie, Roger Trullo, Jun Lian, Caroline Petitjean, Su Ruan, Qian Wang, and Dinggang Shen. Medical image synthesis with context-aware generative adversarial networks. In *Medical Image Computing and Computer Assisted Intervention*, pages 417–425. Springer International Publishing, 2017. URL https://link.springer.com/chapter/10.1007%2F978-3-319-66179-7_48.
- Antoine Plumerault, Hervé Le Borgne, and Céline Hudelot. Controlling generative models with continuous factors of variations. In *International Conference on Machine Learning*, 2020. URL <https://openreview.net/forum?id=H1laeJrKDB>.
- Alec Radford, Luke Metz, and Soumith Chintala. Unsupervised representation learning with deep convolutional generative adversarial networks. In *4th International Conference on Learning Representations*, 2016. URL <http://arxiv.org/abs/1511.06434>.
- Aakash Saboo, Sai Niranjana Ramachandran, Kai Dierkes, and Hacer Yalim Keles. Towards disease-aware image editing of chest x-rays. 2021. URL <https://arxiv.org/abs/2109.01071>.
- Tim Salimans, Ian Goodfellow, Wojciech Zaremba, Vicki Cheung, Alec Radford, Xi Chen, and Xi Chen. Improved techniques for training gans. In *Advances in Neural Information Processing Systems*, volume 29. Curran Associates, Inc., 2016. URL <https://proceedings.neurips.cc/paper/2016/file/8a3363abe792db2d8761d6403605aeb7-Paper.pdf>.
- Veit Sandfort, Ke Yan, Perry J. Pickhardt, and Ronald M. Summers. Data augmentation using generative adversarial networks (CycleGAN) to improve generalizability in CT segmentation tasks. *Scientific Reports*, 9:16884, 2019. URL <https://www.nature.com/articles/s41598-019-52737-x>.
- Yujun Shen and Bolei Zhou. Closed-form factorization of latent semantics in gans. In *IEEE/CVF Conference on Computer Vision and Pattern Recognition*, pages 1532–1540, 2021. URL https://openaccess.thecvf.com/content/CVPR2021/html/Shen_Closed-Form_Factorization_of_Latent_Semantics_in_GANs_CVPR_2021_paper.html.
- Yujun Shen, Jinjin Gu, Xiaoou Tang, and Bolei Zhou. Interpreting the latent space of gans for semantic face editing. In *IEEE/CVF Conference on Computer Vision and Pattern Recognition*, pages 9240–9249, 2020. URL <https://ieeexplore.ieee.org/document/9157070>.
- Hoo-Chang Shin, Neil A. Tenenholtz, Jameson K. Rogers, Christopher G. Schwarz, Matthew L. Senjem, Jeffrey L. Gunter, Katherine P. Andriole, and Mark Michalski. Medical image synthesis for data augmentation and anonymization using generative adversarial networks. In *Simulation and Synthesis in Medical Imaging - Third International Workshop*, volume 11037 of *Lecture Notes in Computer Science*, pages 1–11, 2018. URL https://doi.org/10.1007/978-3-030-00536-8_1.
- Christos Tzelepis, Georgios Tzimiropoulos, and Ioannis Patras. WarpedGANSpace: Finding non-linear rbf paths in GAN latent space. In *IEEE/CVF International Conference on Computer Vision*, pages 6393–6402, October 2021.
- Andrey Voynov and Artem Babenko. Unsupervised discovery of interpretable directions in the GAN latent space. In *Proceedings of the 37th International Conference on Machine Learning*,

- volume 119 of *Proceedings of Machine Learning Research*, pages 9786–9796, 2020. URL <http://proceedings.mlr.press/v119/voynov20a.html>.
- Andrey Voynov, Stanislav Morozov, and Artem Babenko. Object segmentation without labels with large-scale generative models. In *Proceedings of the 38th International Conference on Machine Learning*, volume 139 of *Proceedings of Machine Learning Research*, pages 10596–10606, 2021. URL <https://proceedings.mlr.press/v139/voynov21a.html>.
- Xin Yi, Ekta Walia, and Paul S. Babyn. Generative adversarial network in medical imaging: A review. *Medical Image Analysis*, 58, 2019. URL <https://doi.org/10.1016/j.media.2019.101552>.
- Ronald Yu. A tutorial on vaes: From bayes’ rule to lossless compression. 2020. URL <https://arxiv.org/abs/2006.10273>.
- Qianqian Zhang, Haifeng Wang, Hongya Lu, Daehan Won, and Sang Won Yoon. Medical image synthesis with generative adversarial networks for tissue recognition. In *IEEE International Conference on Healthcare Informatics*, pages 199–207. IEEE Computer Society, 2018. URL <https://doi.org/10.1109/ICHI.2018.00030>.
- Jin Zhu, Guang Yang, and Pietro Lio. How can we make gan perform better in single medical image super-resolution? a lesion focused multi-scale approach. In *IEEE 16th International Symposium on Biomedical Imaging*, pages 1669–1673, 2019. URL <https://ieeexplore.ieee.org/document/8759517>.

Appendix A. Discovered Directions for all Model Configurations.

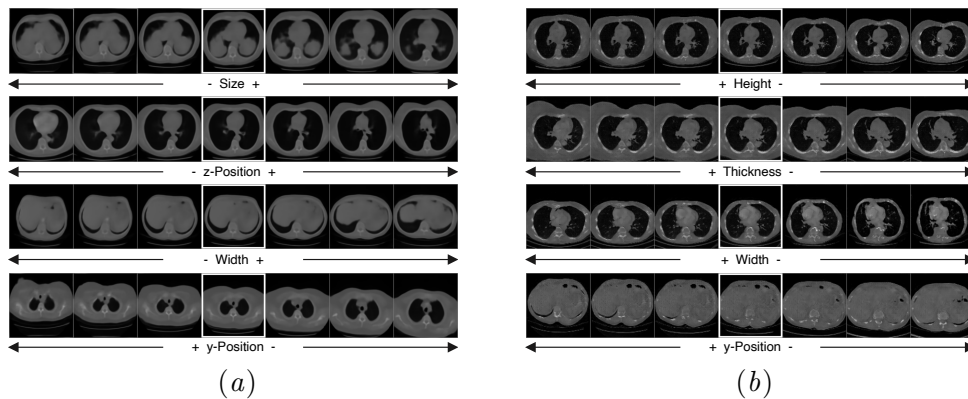


Figure 2: Example of interpretable directions using $A^{32 \times 32}$ with orthonormal columns, LeNet as reconstructor, the VAE (a) and GAN (b) as underlying generative models. The central images correspond to the original latent vector. The images to the left/right of that correspond to a negative/positive shift. We observed fewer disentangled directions than with other methods.

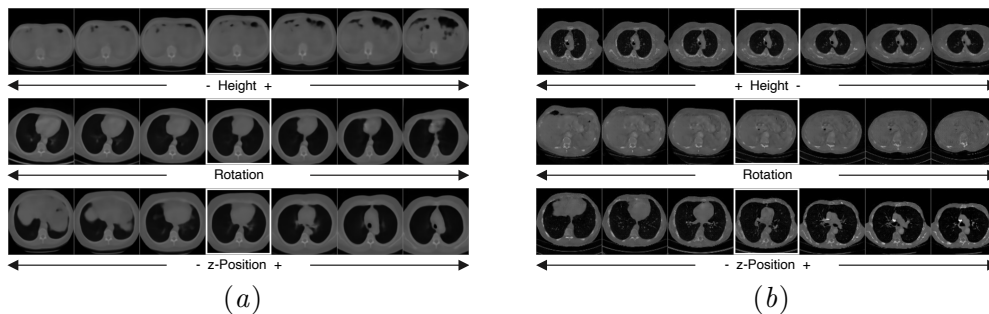


Figure 3: Example of interpretable directions using $A^{32 \times 32}$ with orthonormal columns, ResNet as reconstructor, the VAE (a) and GAN (b) as underlying generative models. The central images correspond to the original latent vector. The images to the left/right of that correspond to a negative/positive shift. Again, we observe far fewer disentangled directions compared to the other methods limiting the amount of directions we report.

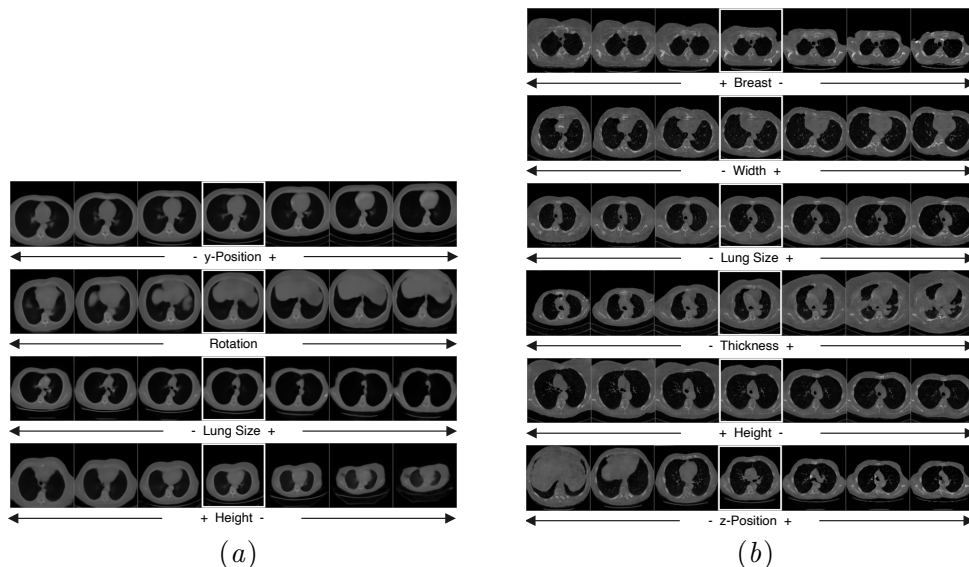


Figure 4: Example of interpretable directions using $A^{32 \times 32}$ with columns of unit length, LeNet as reconstructer, the VAE (a) and GAN (b) as underlying generative models. The central images correspond to the original latent vector. The images to the left/right of that correspond to a negative/positive shift.

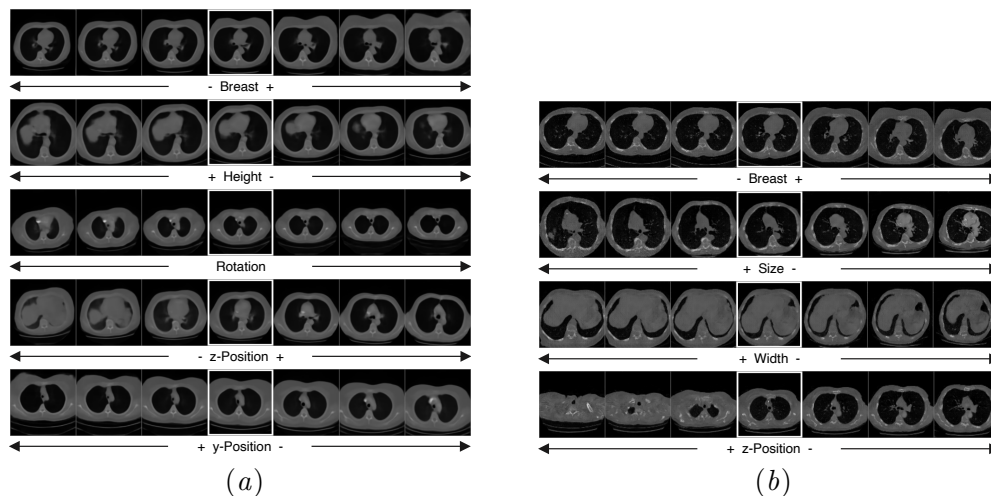


Figure 5: Example of interpretable directions using $A^{32 \times 32}$ with columns of unit length, ResNet as reconstructer, the VAE (a) and GAN (b) as underlying generative models. The central images correspond to the original latent vector. The images to the left/right of that correspond to a negative/positive shift.

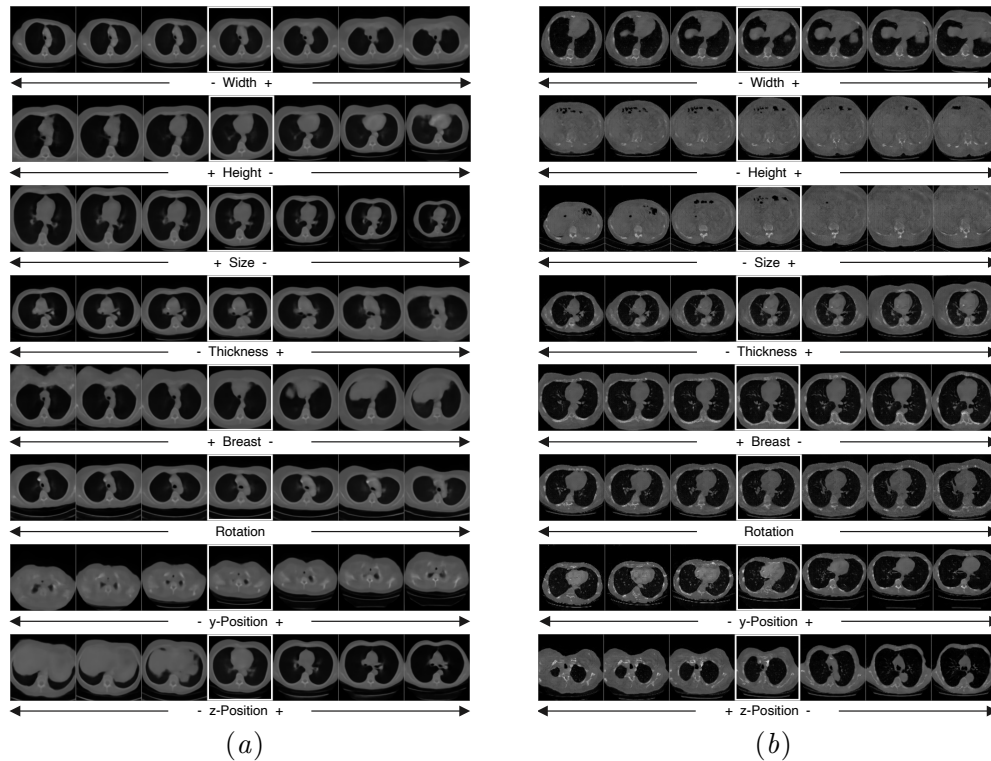


Figure 6: Example of interpretable directions using $A^{32 \times 100}$ with columns of unit length, ResNet as reconstructor, the VAE (a) and GAN (b) as underlying generative models. The central images correspond to the original latent vector. The images to the left/right of that correspond to a negative/positive shift.

Appendix B. Supplementary Images

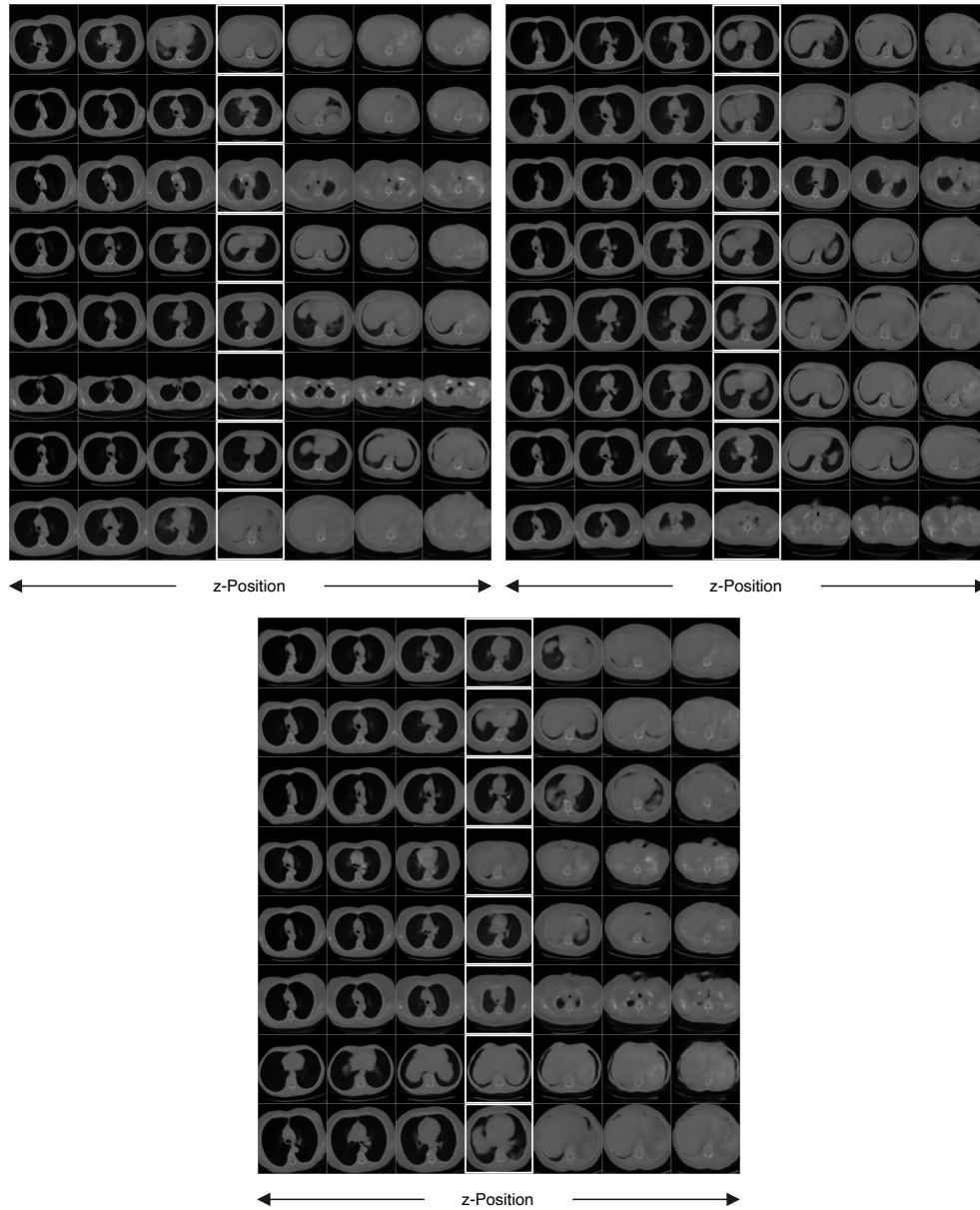


Figure 7: 24 Randomly sampled latent vectors shifted along the directions corresponding to z -Position. The central images correspond to the original latent vector. The images to the left/right of that correspond to a negative/positive shift. Each latent vector shows biological variation and all shifts show realistic changes in anatomy corresponding to different z -positions in order of the amount of shift, such as different anatomical areas of the airways, heart, lungs, and liver.

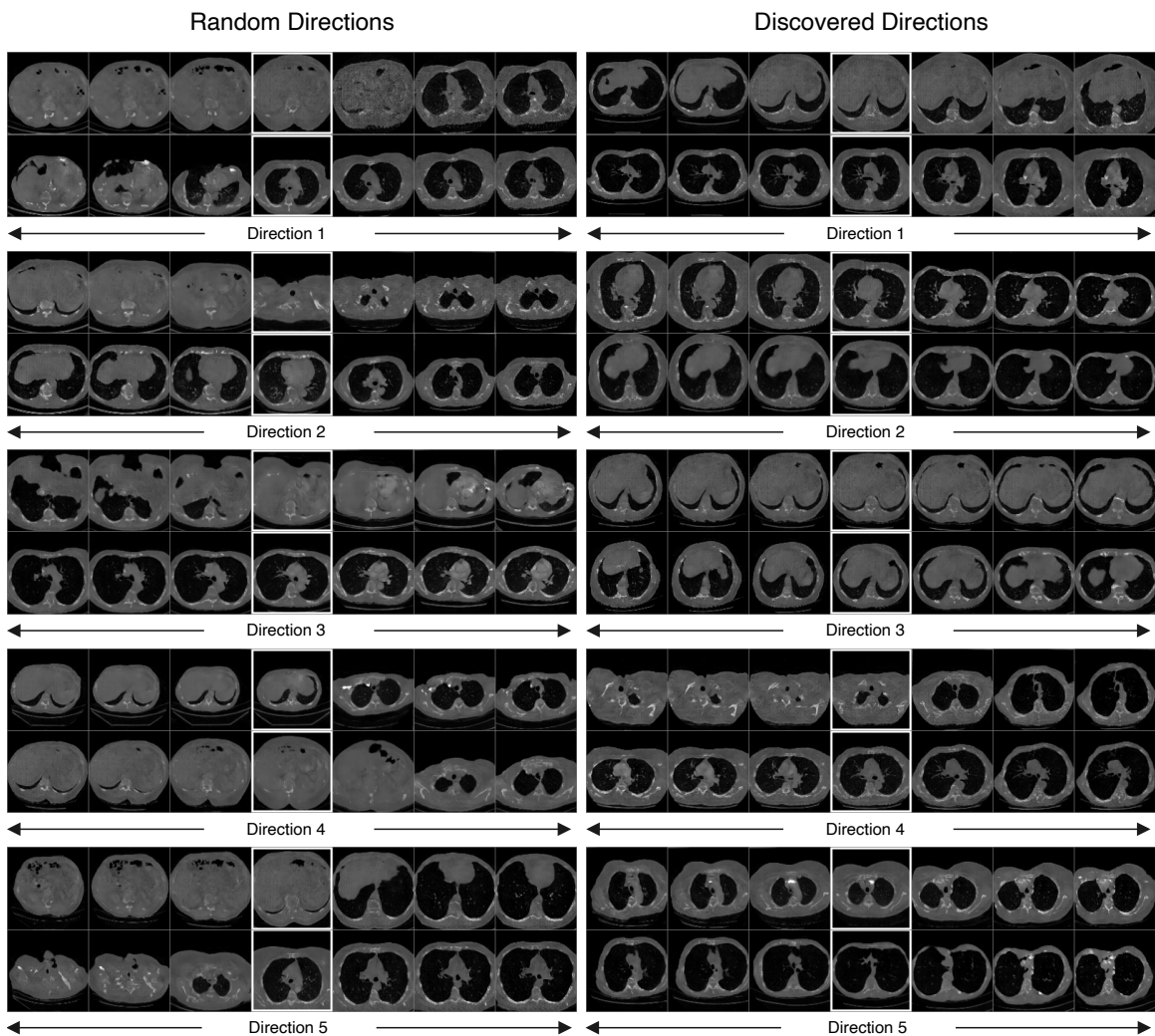


Figure 8: 5 Random directions (left) next to the first 5 discovered directions (right) using $A^{32 \times 100}$ with columns of unit length, LeNet as reconstructor and the GAN as underlying generative model. The central images correspond to the original latent vector. The images to the left/right of that correspond to a negative/positive shift. The results show a marked difference in interpretability of the discovered directions in contrast to random directions.

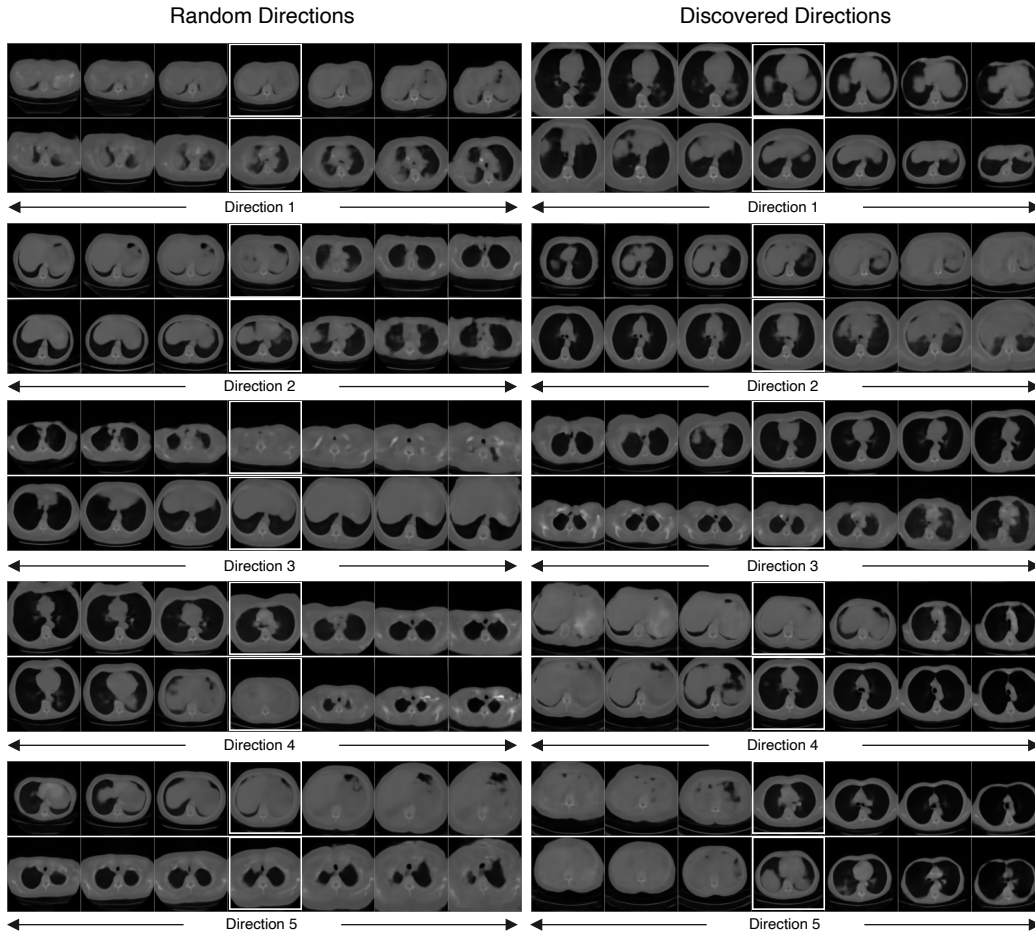


Figure 9: 5 Random directions (left) next to the first 5 discovered directions (right) using $A^{32 \times 100}$ with columns of unit length, LeNet as reconstructor and the VAE as underlying generative model. The central images correspond to the original latent vector. The images to the left/right of that correspond to a negative/positive shift. We can see that the random directions are continuous and some of them somewhat interpretable. In particular, the random direction results are better than what we observe with the GAN. This is most likely due to the regularization of the latent space as well as the VAE learning a structured latent space which is in contrast to the GAN.

Appendix C. Memorization

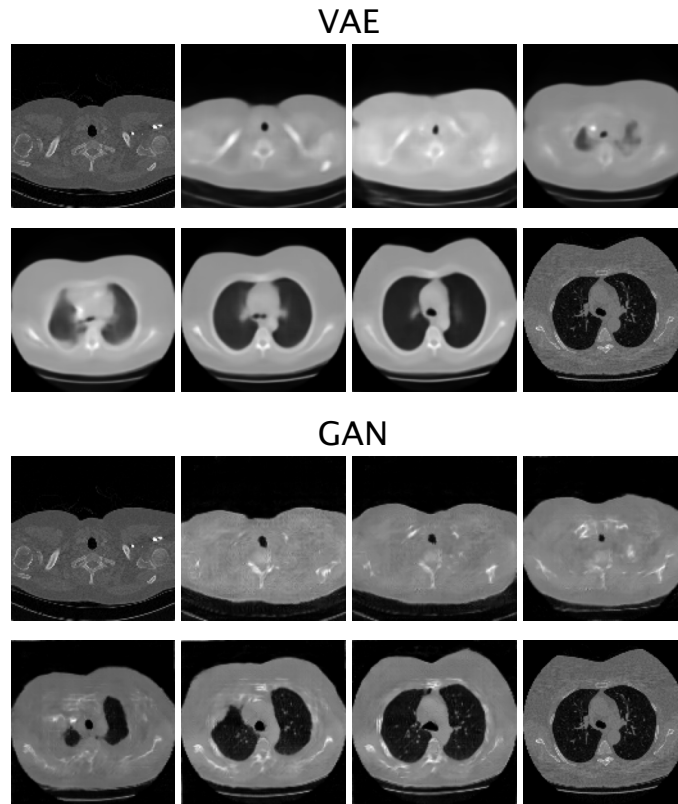


Figure 10: When considering generative latent models, memorization is a concern. To address this, we embed two random images from hold out data (original images are in the top left and bottom right) using reverse latent vector search [Fernández Blanco et al. \(2021\)](#) for the GAN and the encoder for the VAE and move between the two resulting latent vectors to investigate the smoothness of the latent space. As can be seen, the resulting images appear anatomically correct, and interpolation is smooth, indicating that the generative models are not memorizing the data.